Neutrino and Nuclear Properties from Coherent Elastic Neutrino-Nucleus Scattering

Carlo Giunti

INFN, Torino, Italy

Seminar at Pisa, 16 January 2020

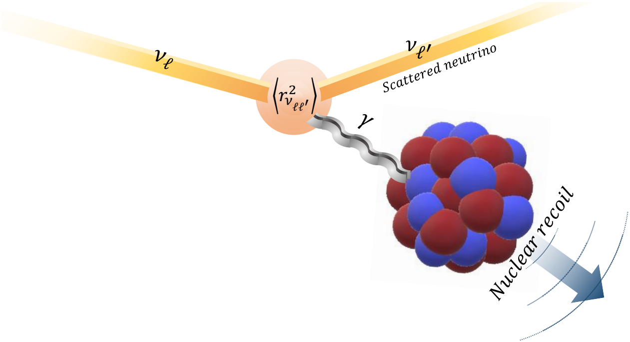

Coherent Elastic Neutrino-Nucleus Scattering

- Predicted in 1974 for $|\vec{q}|R \lesssim 1$
  [Freedman, PRD 9 (1974) 1389]
- $\dfrac{d\sigma}{dT}(E_\nu, T) \sim \dfrac{G_F^2 M}{4\pi} N^2$ [Drukier, Stodolski, PRD (1984) 2295]
- Observed in 2017 in the COHERENT experiment at the Oak Ridge Spallation Neutron Source with CsI ($N_{Cs} = 78$, $N_I = 74$)
  [Science 357 (2017) 1123, arXiv:1708.01294]

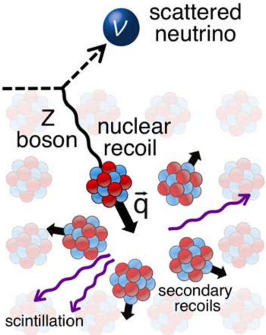

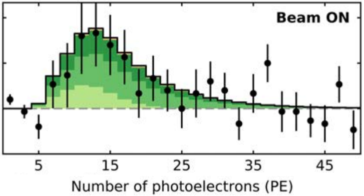

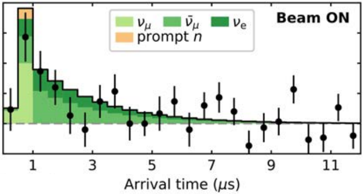

- Several oncoming new experiments: CONUS, CONNIE, NU-CLEUS, MINER, Ricochet, TEXONO, νGEN

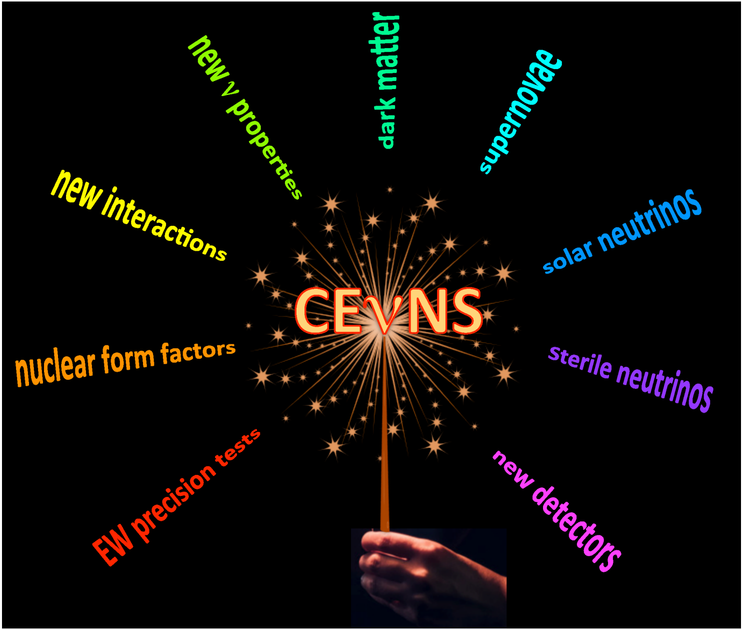

[E. Lisi, Neutrino 2018]

- Taking into account interactions with both neutrons and protons

$$\frac{d\sigma}{dT}(E_\nu, T) = \frac{G_F^2 M}{\pi}\left(1 - \frac{MT}{2E_\nu^2}\right)\left[g_V^n N F_N(|\vec{q}|^2) + g_V^p Z F_Z(|\vec{q}|^2)\right]^2$$

$$g_V^n = -\frac{1}{2} \qquad g_V^p = \frac{1}{2} - 2\sin^2\vartheta_W = 0.0227 \pm 0.0002$$

The neutron contribution is dominant! $\Longrightarrow$ $\frac{d\sigma}{dT} \sim N^2 F_N^2(|\vec{q}|^2)$

- The form factors $F_N(|\vec{q}|^2)$ and $F_Z(|\vec{q}|^2)$ describe the loss of coherence for $|\vec{q}|R \gtrsim 1$. [see: Bednyakov, Naumov, arXiv:1806.08768]

- Coherence requires very small values of the nuclear kinetic recoil energy $T \simeq |\vec{q}|^2/2M$:

$$|\vec{q}|R \lesssim 1 \quad \Longleftrightarrow \quad T \lesssim \frac{1}{2MR^2}$$

$$M \approx 100\,\text{GeV}, \quad R \approx 5\,\text{fm} \quad \Longrightarrow \quad T \lesssim 10\,\text{keV}$$

The COHERENT Experiment

Oak Ridge Spallation Neutron Source

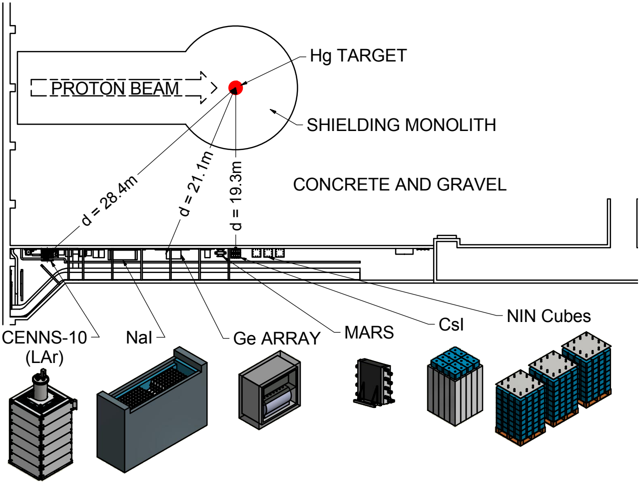

14.6 kg CsI
scintillating crystal

[COHERENT, arXiv:1803.09183]

Neutrino Production at the SNS

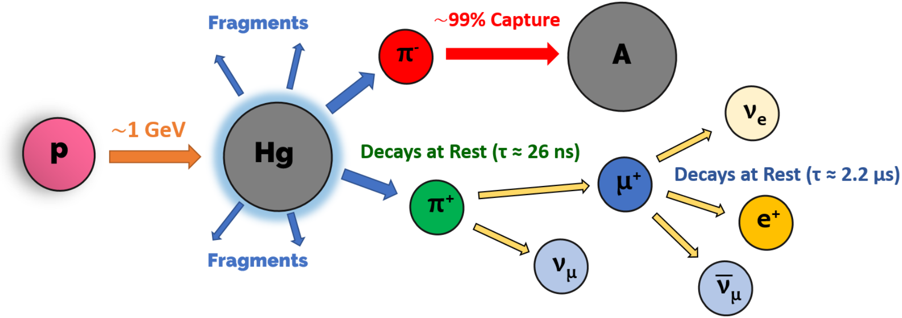

[M. Green @ Magnificent CEvNS 2019]

COHERENT Neutrino Spectrum

Neutrinos at the Oak Ridge Spallation Neutron Source are produced by a pulsed proton beam striking a mercury target.

- Prompt monochromatic ν_μ from stopped pion decays:

$$\pi^+ \to \mu^+ + \nu_\mu$$

$$\frac{dN_{\nu_\mu}}{dE_\nu} = \eta\,\delta\left(E_\nu - \frac{m_\pi^2 - m_\mu^2}{2m_\pi}\right)$$

- Delayed $\bar{\nu}_\mu$ and ν_e from the subsequent muon decays:

$$\mu^+ \to e^+ + \bar{\nu}_\mu + \nu_e$$

$$\frac{dN_{\nu_{\bar{\mu}}}}{dE_\nu} = \eta\,\frac{64E_\nu^2}{m_\mu^3}\left(\frac{3}{4} - \frac{E_\nu}{m_\mu}\right)$$

$$\frac{dN_{\nu_e}}{dE_\nu} = \eta\,\frac{192E_\nu^2}{m_\mu^3}\left(\frac{1}{2} - \frac{E_\nu}{m_\mu}\right)$$

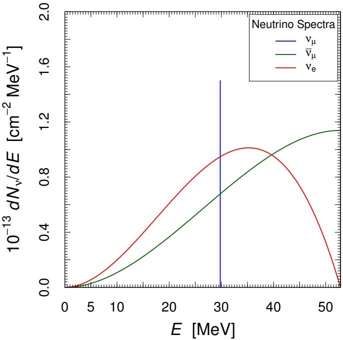

- From kinematics $T < 2E_\nu^2/M$
- $E_\nu \leq \frac{m_\mu}{2} \simeq 52.8\,\mathrm{MeV}$

$$\Downarrow$$

$$T \lesssim 50\,\mathrm{keV}$$

Cross Section

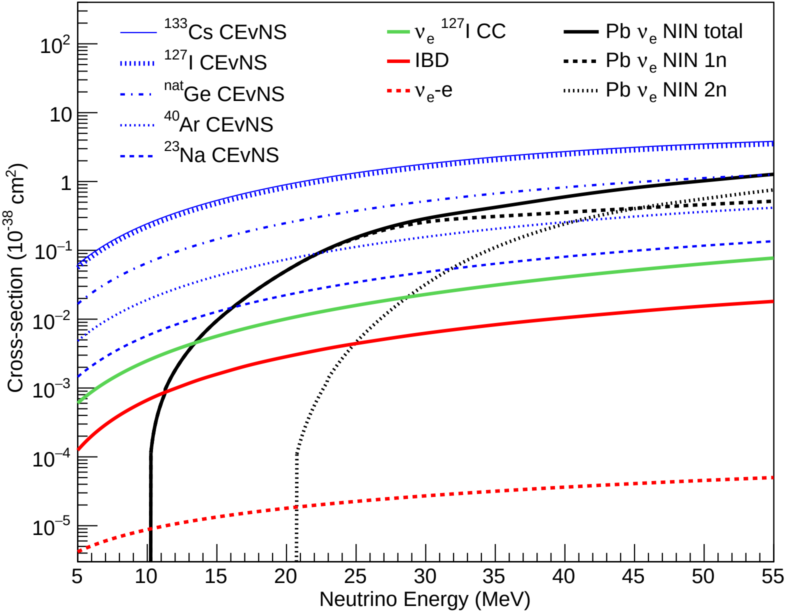

[COHERENT, arXiv:1803.09183]

- In the COHERENT experiment neutrino-nucleus scattering is not completely coherent:

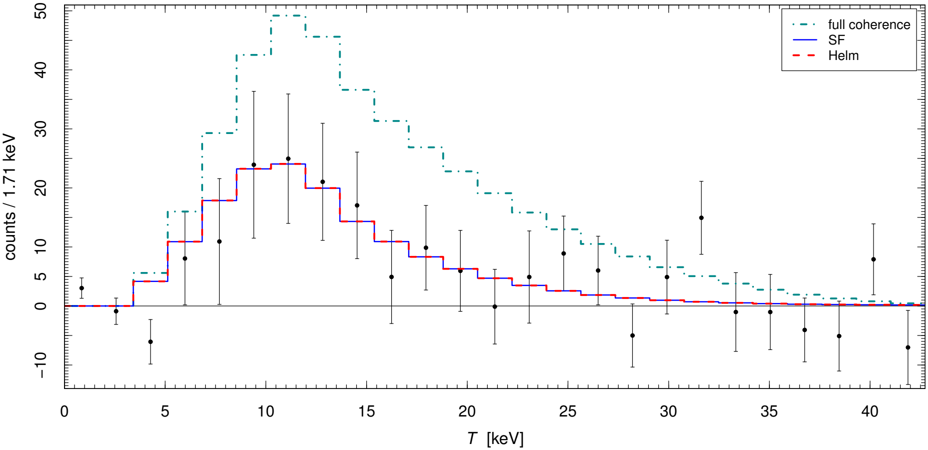

[Cadeddu, CG, Y.F. Li, Y.Y. Zhang, PRL 120 (2018) 072501, arXiv:1710.02730]

- Partial coherency gives information on the nuclear neutron form factor $F_N(|\vec{q}|^2)$, which is the Fourier transform of the neutron distribution in the nucleus.

Helm form factor: $F_N^{\text{Helm}}(|\vec{q}|^2) = 3\,\frac{j_1(|\vec{q}|R_0)}{|\vec{q}|R_0}\,e^{-|\vec{q}|^2 s^2/2}$

Spherical Bessel function of order one: $j_1(x) = \sin(x)/x^2 - \cos(x)/x$

Obtained from the convolution of a sphere with constant density with radius R_0 and a gaussian density with standard deviation s

Rms radius: $R^2 = \langle r^2 \rangle = \frac{3}{5}\,R_0^2 + 3s^2$ Surface thickness: $s \simeq 0.9\,\text{fm}$

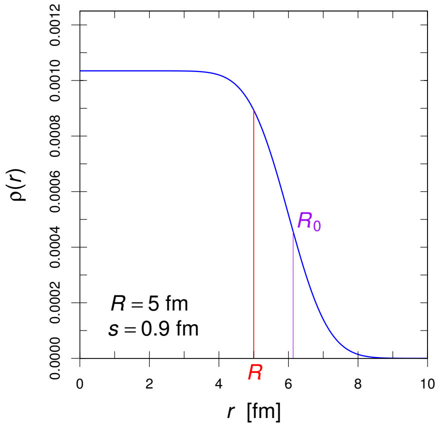

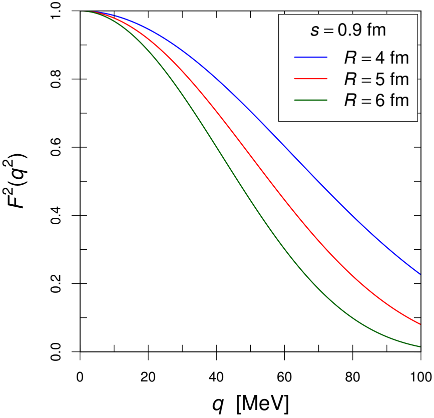

Helm form factor: $F_N^{\text{Helm}}(|\vec{q}|^2) = 3\,\frac{j_1(|\vec{q}|R_0)}{|\vec{q}|R_0}\,e^{-|\vec{q}|^2 s^2/2}$

Spherical Bessel function of order one: $j_1(x) = \sin(x)/x^2 - \cos(x)/x$

Obtained from the convolution of a sphere with constant density with radius R_0 and a gaussian density with standard deviation s

Rms radius: $R^2 = \langle r^2 \rangle = \frac{3}{5}R_0^2 + 3s^2$ Surface thickness: $s \simeq 0.9\,\text{fm}$

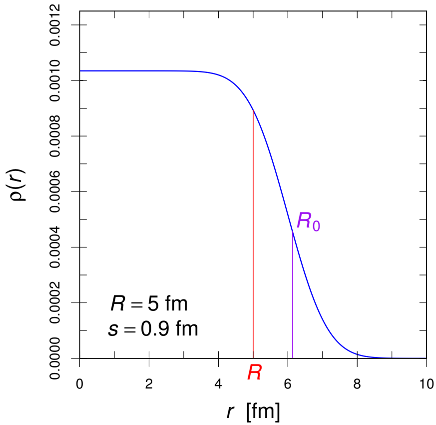

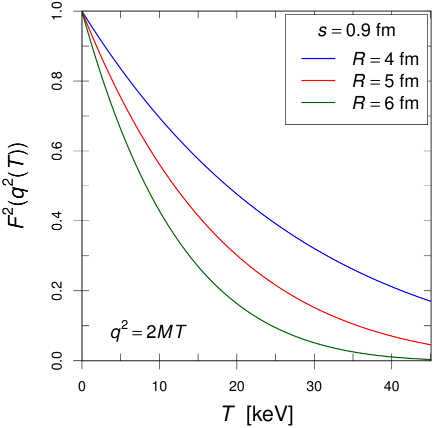

The Nuclear Proton and Neutron Distributions

- The nuclear proton distribution (charge density) is probed with electromagnetic interactions.
- Most sensitive are electron-nucleus elastic scattering and muonic atom spectroscopy.
- Hadron scattering experiments give information on the nuclear neutron distribution, but their interpretation depends on the model used to describe non-perturbative strong interactions.
- More reliable are neutral current weak interaction measurements.
  But they are more difficult.
- Before 2017 there was only one measurement of R_n with neutral-current weak interactions through parity-violating electron scattering:

$$R_n(^{208}\mathrm{Pb}) = 5.78^{+0.16}_{-0.18}\,\mathrm{fm}$$

[PREX, PRL 108 (2012) 112502]

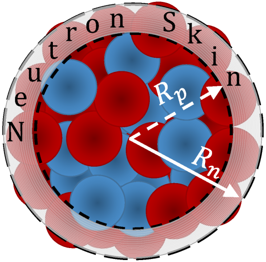

- The rms radii of the proton distributions of ^{133}Cs and ^{127}I have been determined with muonic atom spectroscopy: [Fricke et al, ADNDT 60 (1995) 177]

$$R_p^{(\mu)}(^{133}\text{Cs}) = 4.804\,\text{fm} \qquad R_p^{(\mu)}(^{127}\text{I}) = 4.749\,\text{fm}$$

- Fit of the COHERENT data to get $R_n(^{133}\text{Cs}) \simeq R_n(^{127}\text{I})$:

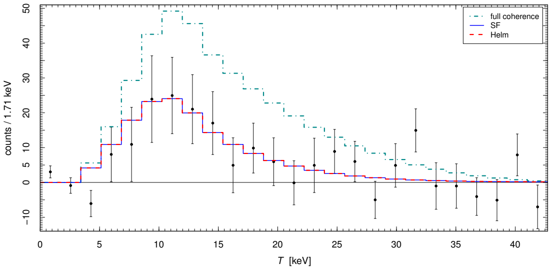

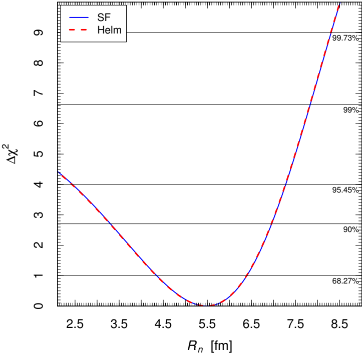

[Cadeddu, Giunti, Li, Zhang, PRL 120 (2018) 072501, arXiv:1710.02730]

$$R_n(^{133}\mathrm{Cs}) \simeq R_n(^{127}\mathrm{I}) = 5.5^{+0.9}_{-1.1}\ \mathrm{fm}$$

[Cadeddu, Giunti, Li, Zhang, PRL 120 (2018) 072501, arXiv:1710.02730]

- This is the first determination of R_n with neutrino-nucleus scattering.
- The uncertainty is large, but it can be improved in future.
- Predictions of nonrelativistic Skyrme-Hartree-Fock (SHF) and relativistic mean field (RMF) nuclear models:

	^{133}Cs		^{127}I	
	R_p	R_n	R_p	R_n
SHF SkM*	4.76	4.90	4.71	4.84
SHF SkP	4.79	4.91	4.72	4.84
SHF SkI4	4.73	4.88	4.67	4.81
SHF Sly4	4.78	4.90	4.71	4.84
SHF UNEDF1	4.76	4.90	4.68	4.83
RMF NL-SH	4.74	4.93	4.68	4.86
RMF NL3	4.75	4.95	4.69	4.89
RMF NL-Z2	4.79	5.01	4.73	4.94
Exp. (μ-atom spect.)	4.804		4.749	

The quenching factor

- The nuclear recoil energy is measured by counting photoelectrons:

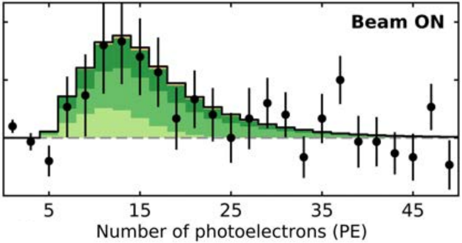

- Light yield was measured well with ^{241}Am and ^{133}Ba gamma sources:

$$Y_L = 13.35 \, N_{PE}/\text{keV}$$

- The nuclear recoil kinetic energy T is connected to N_{PE} by

$$N_{PE} = f_Q(T) \, Y_L \, T$$

- $f_Q(T)$ is the quenching factor, that is difficult to measure.

Old and new quenching factors

- Old quenching factor: COHERENT Collaboration, arXiv:1708.01294
- New quenching factor: Collar, Kavner, Lewis, arXiv:1907.04828

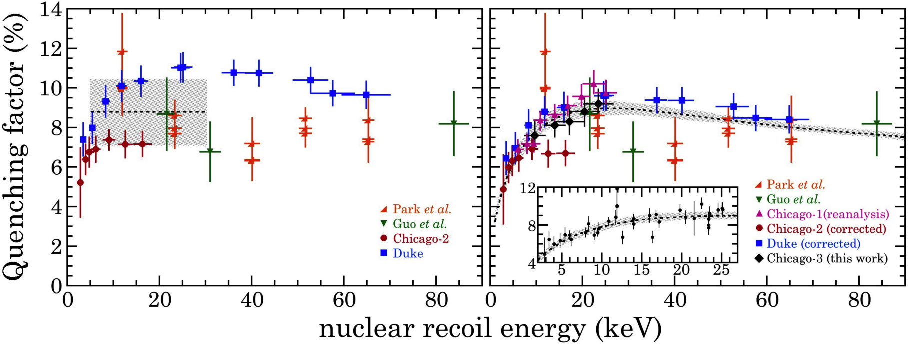

Radius of the neutron distribution

[Cadeddu, Dordei, Giunti, Y.F. Li, Y.Y. Zhang, arXiv:1908.06045]

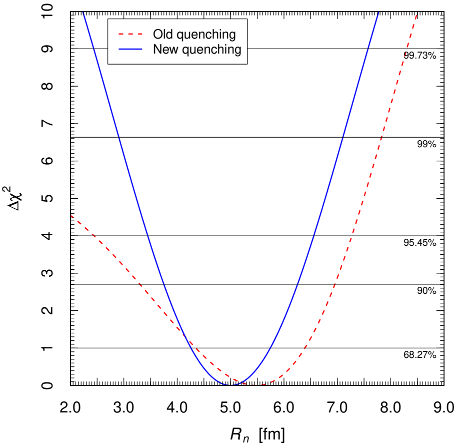

See also: D. Papoulias, arXiv:1907.11644
A. Khan, W. Rodejohann, arXiv:1907.12444

- Old QF: $R_n = 5.5^{+0.9}_{-1.1}\,\text{fm}$
- New QF: $R_n = 5.0 \pm 0.7\,\text{fm}$
  In better agreement with nuclear model calculations.
- New QF is smaller at low T, i.e. low N_{PE}, where the fit of the data needs coherency.

$$N_{\text{PE}} = f_{\text{Q}}(T)\, Y_{\text{L}}\, T$$

- For smaller $f_{\text{Q}}(T)$, a given N_{PE} corresponds to a larger T, which implies a larger $|\vec{q}|$.
- The coherency condition

$$|\vec{q}| R_n \lesssim 1$$

is obtained for smaller R_n.

Weak Mixing Angle from Atomic Parity Violation

[Cadeddu, Dordei, PRD 99 (2019) 033010; Cadeddu et al, arXiv:1908.06045]

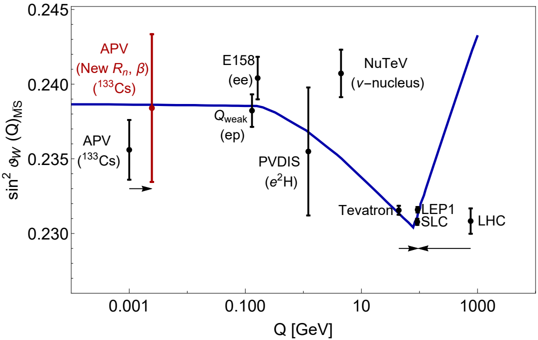

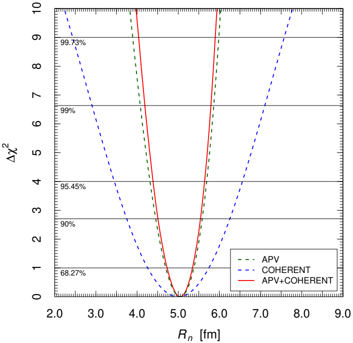

$$Q_W \simeq q_p Z \left(1 - 4\sin^2\vartheta_W\right) - q_n N$$

COHERENT + APV

$\sin^2\vartheta_W = 0.23857(5)$ $\Longrightarrow$ $\begin{cases} R_n = 5.04 \pm 0.31\,\text{fm} \\ \Delta R_{np} = 0.23 \pm 0.31\,\text{fm} \end{cases}$ neutron skin

Neutrino Electromagnetic Interactions

- Effective Hamiltonian: $\mathcal{H}_{\text{em}}^{(\nu)}(x) = j_{\mu}^{(\nu)}(x) A^{\mu}(x) = \sum_{k,j=1} \overline{\nu_k}(x) \Lambda_{\mu}^{kj} \nu_j(x) A^{\mu}(x)$

- Effective electromagnetic vertex:

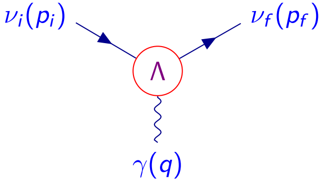

$$\langle \nu_f(p_f) | j_{\mu}^{(\nu)}(0) | \nu_i(p_i) \rangle = \overline{u_f}(p_f) \Lambda_{\mu}^{fi}(q) u_i(p_i)$$

$$q = p_i - p_f$$

- Vertex function:

$$\Lambda_{\mu}(q) = \left(\gamma_{\mu} - q_{\mu} \not{q}/q^2\right) \left[F_Q(q^2) + F_A(q^2) q^2 \gamma_5\right] - i \sigma_{\mu\nu} q^{\nu} \left[F_M(q^2) + i F_E(q^2) \gamma_5\right]$$

Lorentz-invariant form factors: charge (F_Q), anapole (F_A), magnetic (F_M), electric (F_E)

$q^2 = 0 \implies$ q (charge), a (anapole), μ (magnetic), ε (electric)

helicity-conserving: q, a — helicity-flipping: μ, ε

Electromagnetic Vertex Function

$$\Lambda_\mu(q) = \left(\gamma_\mu - q_\mu \not{q}/q^2\right)\left[F_Q(q^2) + F_A(q^2) q^2 \gamma_5\right] - i\sigma_{\mu\nu} q^\nu \left[F_M(q^2) + i F_E(q^2)\gamma_5\right]$$

Lorentz-invariant form factors: charge (F_Q), anapole (F_A), magnetic (F_M), electric (F_E)

$q^2 = 0 \implies$ charge → q, anapole → a, magnetic → μ, electric → ε

- Hermitian form factors: $F_Q = F_Q^\dagger$, $F_A = F_A^\dagger$, $F_M = F_M^\dagger$, $F_E = F_E^\dagger$
- Majorana neutrinos: $F_Q = -F_Q^T$, $F_A = F_A^T$, $F_M = -F_M^T$, $F_E = -F_E^T$

no diagonal charges and electric and magnetic moments in the mass basis

- For left-handed ultrarelativistic neutrinos $\gamma_5 \to -1 \Rightarrow$ The phenomenology of the charge and anapole moments are similar and the phenomenology of the magnetic and electric moments are similar.
- For ultrarelativistic neutrinos the charge and anapole terms conserve helicity, whereas the magnetic and electric terms invert helicity.

Neutrino Charge Radius

- In the Standard Model neutrinos are neutral and there are no electromagnetic interactions at the tree-level.

- Radiative corrections generate an effective electromagnetic interaction vertex

$$\Lambda_\mu(q) = \left(\gamma_\mu - q_\mu \not{q}/q^2\right) F(q^2)$$

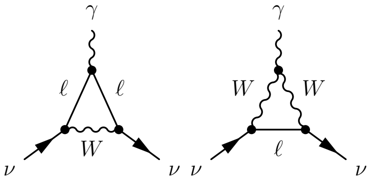

- $F(q^2) = \cancel{F(0)} + q^2 \left.\frac{dF(q^2)}{dq^2}\right|_{q^2=0} + \ldots = q^2 \frac{\langle r^2 \rangle}{6} + \ldots$

- In the Standard Model: [Bernabeu et al, PRD 62 (2000) 113012, NPB 680 (2004) 450]

$$\langle r^2_{\nu_\ell} \rangle_{\text{SM}} = -\frac{G_F}{2\sqrt{2}\pi^2}\left[3 - 2\log\left(\frac{m_\ell^2}{m_W^2}\right)\right]$$

$$\langle r^2_{\nu_e} \rangle_{\text{SM}} = -8.2 \times 10^{-33}\,\text{cm}^2$$
$$\langle r^2_{\nu_\mu} \rangle_{\text{SM}} = -4.8 \times 10^{-33}\,\text{cm}^2$$
$$\langle r^2_{\nu_\tau} \rangle_{\text{SM}} = -3.0 \times 10^{-33}\,\text{cm}^2$$

Experimental Bounds

Method	Experiment	Limit [cm^2]	CL	Year
Reactor $\bar{\nu}_e\, e^-$	Krasnoyarsk	$\lvert\langle r^2_{\nu_e}\rangle\rvert < 7.3 \times 10^{-32}$	90%	1992
	TEXONO	$-4.2 \times 10^{-32} < \langle r^2_{\nu_e}\rangle < 6.6 \times 10^{-32}$	90%	2009
Accelerator $\nu_e\, e^-$	LAMPF	$-7.12 \times 10^{-32} < \langle r^2_{\nu_e}\rangle < 10.88 \times 10^{-32}$	90%	1992
	LSND	$-5.94 \times 10^{-32} < \langle r^2_{\nu_e}\rangle < 8.28 \times 10^{-32}$	90%	2001
Accelerator $\nu_\mu\, e^-$	BNL-E734	$-5.7 \times 10^{-32} < \langle r^2_{\nu_\mu}\rangle < 1.1 \times 10^{-32}$	90%	1990
	CHARM-II	$\lvert\langle r^2_{\nu_\mu}\rangle\rvert < 1.2 \times 10^{-32}$	90%	1994

[see the review Giunti, Studenikin, RMP 87 (2015) 531, arXiv:1403.6344

and the update in Cadeddu, Giunti, Kouzakov, Y.F. Li, Studenikin, Y.Y. Zhang, PRD 98 (2018) 113010, arXiv:1810.05606]

- Neutrino charge radii contributions to ν_ℓ–$\mathcal{N}$ CEνNS:

$$\frac{d\sigma_{\nu_\ell\text{-}\mathcal{N}}}{dT}(E_\nu, T) = \frac{G_F^2 M}{\pi}\left(1 - \frac{MT}{2E_\nu^2}\right)\left\{\left[\underbrace{-\frac{1}{2}}_{g_V^n} N F_N(|\vec{q}|^2) + \left(\underbrace{\frac{1}{2} - 2\sin^2\vartheta_W}_{g_V^p \simeq 0.023} - \frac{2}{3}\, m_W^2 \sin^2\vartheta_W \langle r^2_{\nu_{\ell\ell}}\rangle\right) Z F_Z(|\vec{q}|^2)\right]^2 + \frac{4}{9}\, m_W^4 \sin^4\vartheta_W Z^2 F_Z^2(|\vec{q}|^2) \sum_{\ell'\neq\ell} |\langle r^2_{\nu_{\ell'\ell}}\rangle|^2\right\}$$

- In the Standard Model there are only diagonal charge radii $\langle r^2_{\nu_\ell}\rangle \equiv \langle r^2_{\nu_{\ell\ell}}\rangle$ because lepton numbers are conserved.

- Diagonal charge radii generate the coherent shifts

$$\sin^2\vartheta_W \to \sin^2\vartheta_W\left(1 + \frac{1}{3} m_W^2 \langle r^2_{\nu_\ell}\rangle\right) \quad \Longleftrightarrow \quad \nu_\ell + \mathcal{N} \to \nu_\ell + \mathcal{N}$$

- Transition charge radii generate the incoherent contribution

$$\frac{4}{9}\, m_W^4 \sin^4\vartheta_W Z^2 F_Z^2(|\vec{q}|^2) \sum_{\ell'\neq\ell} |\langle r^2_{\nu_{\ell'\ell}}\rangle|^2 \quad \Longleftrightarrow \quad \nu_\ell + \mathcal{N} \to \sum_{\ell'\neq\ell} \nu_{\ell'\neq\ell} + \mathcal{N}$$

[Kouzakov, Studenikin, PRD 95 (2017) 055013, arXiv:1703.00401]

COHERENT Neutrino Spectrum and Time

- Neutrinos at the Oak Ridge Spallation Neutron Source are produced by a pulsed proton beam striking a mercury target.
- Prompt monochromatic ν_μ from stopped pion decays:
$$\pi^+ \to \mu^+ + \nu_\mu$$
- Delayed $\bar{\nu}_\mu$ and ν_e from the subsequent muon decays:
$$\mu^+ \to e^+ + \bar{\nu}_\mu + \nu_e$$
- The COHERENT energy and time information allow us to distinguish the interactions of ν_e, ν_μ, and $\bar{\nu}_\mu$.
- Note that $\langle r^2_{\bar{\nu}_{\ell\ell'}} \rangle = -\langle r^2_{\nu_{\ell\ell'}} \rangle$, but also $g_V^{p,n}(\bar{\nu}) = -g_V^{p,n}(\nu)$.

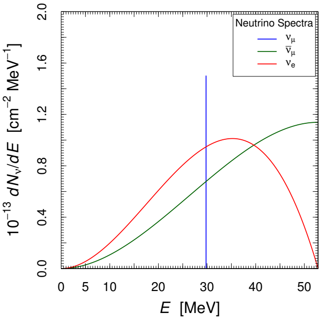

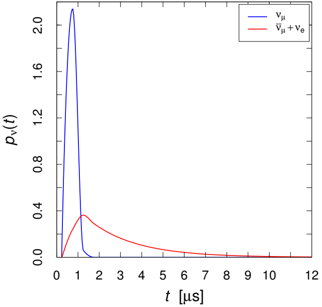

Fits with the old and new quenching factors

[Cadeddu, Dordei, Giunti, Y.F. Li, Y.Y. Zhang, arXiv:1908.06045]

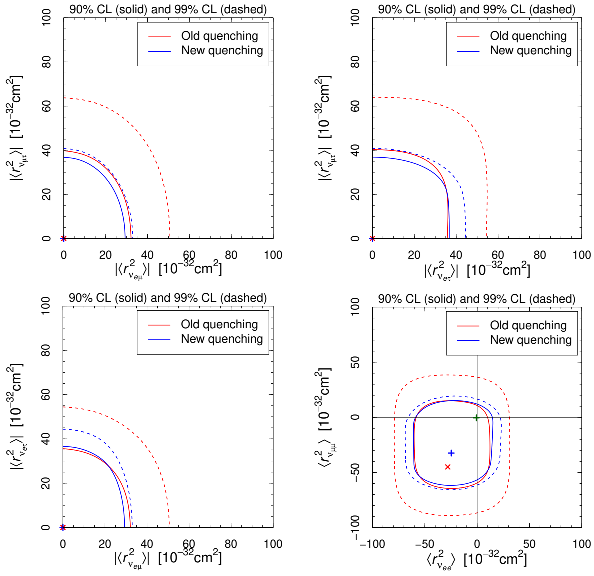

- Free neutron distribution radii $R_n(^{133}\mathrm{Cs})$, $R_n(^{127}\mathrm{I})$.
- Slight improvement of 90% CL bounds with the new quenching factor.
- Significant improvement of 99% CL bounds strengthen the statistical reliability.
- The bounds on the diagonal charge radii are still not competitive with other measurements.
- Note the unique bounds on the transition charge radii that were not considered before Cadeddu et al, arXiv:1810.05606.

Fits without transition charge radii

[Cadeddu, Dordei, Giunti, Y.F. Li, Y.Y. Zhang, arXiv:1908.06045]

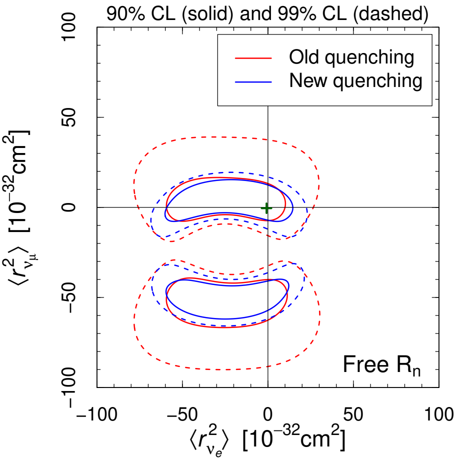

- Motivated by the Standard Model, where there are only diagonal charge radii.
- Explanation of the excluded area in the middle:
  - The cross section contribution of a diagonal charge radius $\langle r^2_{\nu_\ell} \rangle$ approximately cancel the weak neutral current contributions for

$$\langle r^2_{\nu_\ell} \rangle \simeq -\frac{3\,N}{4\,Z\,m_W^2 \sin^2\vartheta_W} \simeq -26 \times 10^{-32}\,\text{cm}^2$$

  - Around this value the cross section is strongly suppressed and cannot fit the COHERENT data.

Neutrino Electric Charges

- Neutrinos can be millicharged particles in theories beyond the Standard Model.

- Neutrino charge contributions to ν_ℓ–$\mathcal{N}$ CEνNS:

$$\frac{d\sigma_{\nu_\ell\text{-}\mathcal{N}}}{dT}(E_\nu, T) = \frac{G_F^2 M}{\pi}\left(1 - \frac{MT}{2E_\nu^2}\right)\left\{\left[\underbrace{-\frac{1}{2}}_{g_V^n} N F_N(|\vec{q}|^2) + \left(\underbrace{\frac{1}{2} - 2\sin^2\vartheta_W}_{g_V^p \simeq 0.023} + \frac{2m_W^2 \sin^2\vartheta_W}{MT}\, q_{\nu_{\ell\ell}}\right) Z F_Z(|\vec{q}|^2)\right]^2 + \frac{4m_W^4 \sin^4\vartheta_W}{M^2 T^2}\, Z^2 F_Z^2(|\vec{q}|^2) \sum_{\ell' \neq \ell} |q_{\nu_{\ell\ell'}}|^2\right\}$$

- $q_{\bar{\nu}_{\ell\ell'}} = -q_{\nu_{\ell\ell'}}$, but also $g_V^{p,n}(\bar{\nu}) = -g_V^{p,n}(\nu)$.

Approximate limits on neutrino millicharges

Limit	Method	Reference
$\vert q_{\nu_e}\vert \lesssim 3 \times 10^{-21}\, e$	Neutrality of matter	Raffelt (1999)
$\vert q_{\nu_e}\vert \lesssim 3.7 \times 10^{-12}\, e$	Nuclear reactor	Gninenko et al, (2006)
$\vert q_{\nu_e}\vert \lesssim 1.5 \times 10^{-12}\, e$	Nuclear reactor	Studenikin (2013)
$\vert q_{\nu_\tau}\vert \lesssim 3 \times 10^{-4}\, e$	SLAC e^- beam dump	Davidson et al, (1991)
$\vert q_{\nu_\tau}\vert \lesssim 4 \times 10^{-4}\, e$	BEBC beam dump	Babu et al, (1993)
$\vert q_{\nu}\vert \lesssim 6 \times 10^{-14}\, e$	Solar cooling (plasmon decay)	Raffelt (1999)
$\vert q_{\nu}\vert \lesssim 2 \times 10^{-14}\, e$	Red giant cooling (plasmon decay)	Raffelt (1999)

Neutrality of matter

- From electric charge conservation in neutron beta decay ($n \to p + e^- + \bar{\nu}_e$)

$$q_{\nu_e} = q_n - (q_p + q_e) = \frac{A}{Z}\,(q_n - q_{\text{mat}}) \quad \text{with} \quad q_{\text{mat}} = \frac{Z(q_p + q_e) + N q_n}{A}$$

- $q_{\text{mat}} = (-0.1 \pm 1.1) \times 10^{-21}\, e$ with SF_6, which has $A = 146.06$ and $Z = 70$

[Bressi, et al., PRA 83 (2011) 052101, arXiv:1102.2766]

- $q_n = (-0.4 \pm 1.1) \times 10^{-21}\, e$ [Baumann, Kalus, Gahler, Mampe, PRD 37 (1988) 3107]

- $q_{\nu_e} = (-0.6 \pm 3.2) \times 10^{-21}\, e$ [Giunti, Studenikin, RMP 87 (2015) 531, arXiv:1403.6344]

COHERENT constraints on neutrino millicharges

[Cadeddu, Dordei, Giunti, Y.F. Li, Y.Y. Zhang, arXiv:1908.06045]

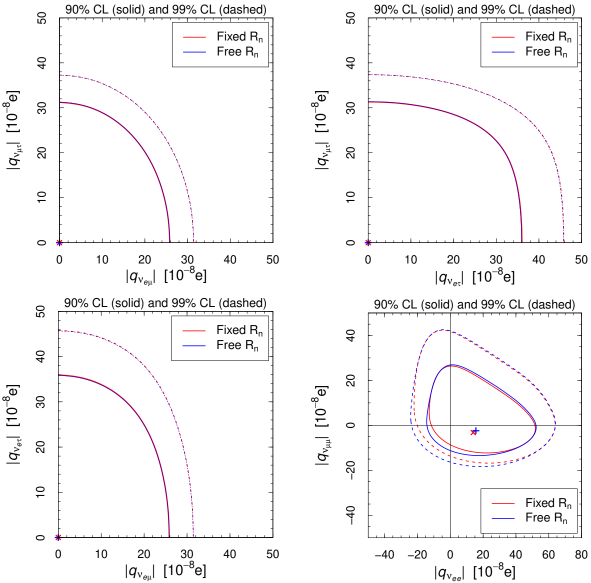

- The bounds on the charges involving the electron neutrino flavor

  $q_{\nu_{ee}}$ $q_{\nu_{e\mu}}$ $q_{\nu_{e\tau}}$

  are not competitive with respect to those obtained in reactor neutrino experiments, that are at the level of $10^{-12}\,e$ in neutrino-electron elastic scattering experiments.

- The bounds on

  $q_{\nu_{\mu\mu}}$ $q_{\nu_{\mu\tau}}$

  are the first ones obtained from laboratory data.

Neutrino Magnetic and Electric Moments

- Extended Standard Model with right-handed neutrinos and $\Delta L = 0$:

$$\mu^{\text{D}}_{kk} \simeq 3.2 \times 10^{-19} \mu_{\text{B}} \left(\frac{m_k}{\text{eV}} \right) \qquad \varepsilon^{\text{D}}_{kk} = 0$$

$$\left. \begin{array}{l} \mu^{\text{D}}_{kj} \\ i\varepsilon^{\text{D}}_{kj} \end{array} \right\} \simeq -3.9 \times 10^{-23} \mu_{\text{B}} \left(\frac{m_k \pm m_j}{\text{eV}} \right) \sum_{\ell=e,\mu,\tau} U^{*}_{\ell k} U_{\ell j} \left(\frac{m_\ell}{m_\tau} \right)^2$$

off-diagonal moments are GIM-suppressed

[Fujikawa, Shrock, PRL 45 (1980) 963; Pal, Wolfenstein, PRD 25 (1982) 766; Shrock, NPB 206 (1982) 359; Dvornikov, Studenikin, PRD 69 (2004) 073001, JETP 99 (2004) 254]

- Extended Standard Model with Majorana neutrinos ($|\Delta L| = 2$):

$$\mu^{\text{M}}_{kj} \simeq -7.8 \times 10^{-23} \mu_{\text{B}} \, i \, (m_k + m_j) \sum_{\ell=e,\mu,\tau} \text{Im}\left[U^{*}_{\ell k} U_{\ell j} \right] \frac{m_\ell^2}{m_W^2}$$

$$\varepsilon^{\text{M}}_{kj} \simeq 7.8 \times 10^{-23} \mu_{\text{B}} \, i \, (m_k - m_j) \sum_{\ell=e,\mu,\tau} \text{Re}\left[U^{*}_{\ell k} U_{\ell j} \right] \frac{m_\ell^2}{m_W^2}$$

[Shrock, NPB 206 (1982) 359]

GIM-suppressed, but additional model-dependent contributions of the scalar sector can enhance the Majorana transition dipole moments

[Pal, Wolfenstein, PRD 25 (1982) 766; Barr, Freire, Zee, PRL 65 (1990) 2626; Pal, PRD 44 (1991) 2261]

$$\left(\frac{d\sigma_{\nu e^-}}{dT_e}\right)_{\text{mag}} = \frac{\pi\alpha^2}{m_e^2}\left(\frac{1}{T_e} - \frac{1}{E_\nu}\right)\left(\frac{\mu_\nu}{\mu_B}\right)^2$$

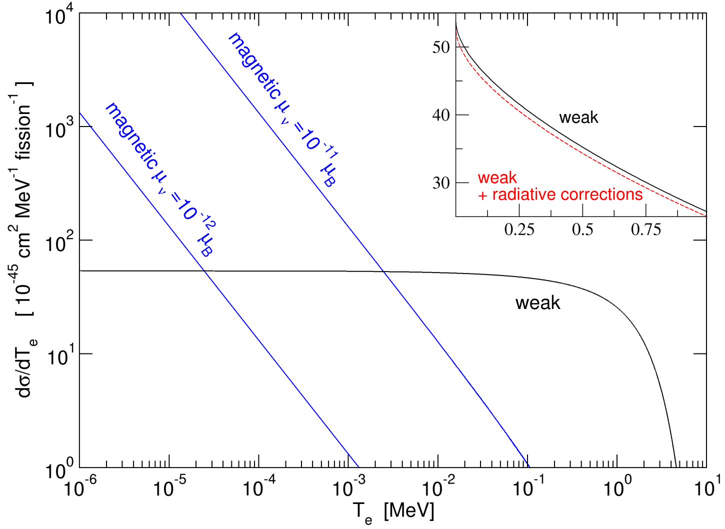

Method	Experiment	Limit $[\mu_B]$	CL	Year
Reactor $\bar{\nu}_e\, e^-$	Krasnoyarsk	$\mu_{\nu_e} < 2.4 \times 10^{-10}$	90%	1992
	Rovno	$\mu_{\nu_e} < 1.9 \times 10^{-10}$	95%	1993
	MUNU	$\mu_{\nu_e} < 9 \times 10^{-11}$	90%	2005
	TEXONO	$\mu_{\nu_e} < 7.4 \times 10^{-11}$	90%	2006
	GEMMA	$\mu_{\nu_e} < 2.9 \times 10^{-11}$	90%	2012
Accelerator $\nu_e\, e^-$	LAMPF	$\mu_{\nu_e} < 1.1 \times 10^{-9}$	90%	1992
Accelerator $(\nu_\mu, \bar{\nu}_\mu)\, e^-$	BNL-E734	$\mu_{\nu_\mu} < 8.5 \times 10^{-10}$	90%	1990
	LAMPF	$\mu_{\nu_\mu} < 7.4 \times 10^{-10}$	90%	1992
	LSND	$\mu_{\nu_\mu} < 6.8 \times 10^{-10}$	90%	2001
Accelerator $(\nu_\tau, \bar{\nu}_\tau)\, e^-$	DONUT	$\mu_{\nu_\tau} < 3.9 \times 10^{-7}$	90%	2001
Solar $\nu_e\, e^-$	Super-Kamiokande	$\mu_S(E_\nu \gtrsim 5\,\text{MeV}) < 1.1 \times 10^{-10}$	90%	2004
	Borexino	$\mu_S(E_\nu \lesssim 1\,\text{MeV}) < 2.8 \times 10^{-11}$	90%	2017

[see the review Giunti, Studenikin, RMP 87 (2015) 531, arXiv:1403.6344]

- Gap of about 8 orders of magnitude between the experimental limits and the $\lesssim 10^{-19}\,\mu_B$ prediction of the minimal Standard Model extensions.
- $\mu_\nu \gg 10^{-19}\,\mu_B$ discovery $\Rightarrow$ non-minimal new physics beyond the SM.
- Neutrino spin-flavor precession in a magnetic field

[Lim, Marciano, PRD 37 (1988) 1368; Akhmedov, PLB 213 (1988) 64]

- Neutrino magnetic (and electric) moment contributions to CEνNS $\nu_\ell + \mathcal{N} \to \sum_{\ell'} \nu_{\ell'} + \mathcal{N}$:

$$\frac{d\sigma_{\nu_\ell\text{-}\mathcal{N}}}{dT}(E_\nu, T) = \frac{G_F^2 M}{\pi} \left(1 - \frac{MT}{2E_\nu^2}\right) \left[g_V^n N F_N(|\vec{q}|^2) + g_V^p Z F_Z(|\vec{q}|^2)\right]^2 + \frac{\pi\alpha^2}{m_e^2} \left(\frac{1}{T} - \frac{1}{E_\nu}\right) Z^2 F_Z^2(|\vec{q}|^2) \sum_{\ell' \neq \ell} \frac{|\mu_{\ell\ell'}|^2}{\mu_B^2}$$

- The magnetic moment interaction adds incoherently to the weak interaction because it flips helicity.
- The m_e is due to the definition of the Bohr magneton: $\mu_B = e/2m_e$.

COHERENT constraints on ν magnetic moments

[Cadeddu, Dordei, Giunti, Y.F. Li, Y.Y. Zhang, arXiv:1908.06045]

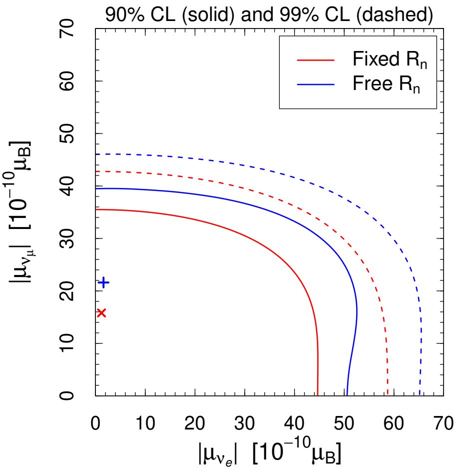

- The sensitivity to $|\mu_{\nu_e}|$ is not competitive with that of reactor experiments:

$$|\mu_{\nu_e}| < 2.9 \times 10^{-11}\,\mu_{\mathrm{B}} \quad (90\%\ \mathrm{CL})$$

[GEMMA, AHEP 2012 (2012) 350150]

- The constraint on $|\mu_{\nu_\mu}|$ is not too far from the best current laboratory limit:

$$|\mu_{\nu_\mu}| < 6.8 \times 10^{-10}\,\mu_{\mathrm{B}} \quad (90\%\ \mathrm{CL})$$

[LSND, PRD 63 (2001) 112001]

Neutrino Non-Standard Interactions

- Non-renormalizable effective NSI of left-handed neutrinos.

- Charged-Current-like NSI: $(\alpha, \beta, \sigma, \delta = e, \mu, \tau)$

$$\mathcal{H}_{\text{NSI}}^{\text{CC}} = 2\sqrt{2} G_{\text{F}} V_{ud} \sum_{\alpha,\beta} \left(\overline{\ell_{\alpha L}} \gamma_\rho \nu_{\beta L} \right) \left[\varepsilon_{\alpha\beta}^{udL} \overline{u_L} \gamma^\rho d_L + \varepsilon_{\alpha\beta}^{udR} \overline{u_R} \gamma^\rho d_R \right] + \text{H.c.}$$
$$+ 2\sqrt{2} G_{\text{F}} \sum_{\alpha,\beta} \left(\overline{\nu_{\alpha L}} \gamma_\rho \nu_{\beta L} \right) \sum_{\sigma \neq \delta} \left[\varepsilon_{\alpha\beta}^{\sigma\delta L} \overline{\ell_{\sigma L}} \gamma^\rho \ell_{\delta L} + \varepsilon_{\alpha\beta}^{\sigma\delta R} \overline{\ell_{\sigma R}} \gamma^\rho \ell_{\delta R} \right]$$

- Neutral-Current-like or Matter NSI: $(\varepsilon_{\alpha\beta}^{fP} = \varepsilon_{\beta\alpha}^{fP*})$

$$\mathcal{H}_{\text{NSI}}^{\text{NC}} = 2\sqrt{2} G_{\text{F}} \sum_{\alpha,\beta} \left(\overline{\nu_{\alpha L}} \gamma_\rho \nu_{\beta L} \right) \sum_{f=e,u,d} \left[\varepsilon_{\alpha\beta}^{fL} \overline{f_L} \gamma^\rho f_L + \varepsilon_{\alpha\beta}^{fR} \overline{f_R} \gamma^\rho f_R \right]$$

- The ε couplings weight the NSI with respect to SM CC and NC weak interactions.

- NSI are obtained in Effective Field Theory from operators of dimension 6 and higher:

$$\begin{aligned}\mathscr{O}_6 \;=\; & \sum_{\alpha,\beta,\sigma,\delta} C^{1}_{\alpha\beta\sigma\delta} \left(\overline{L_\alpha}\gamma^\rho L_\beta\right)\left(\overline{L_\sigma}\gamma_\rho L_\delta\right) \\ & + \sum_{\alpha,\beta,\sigma,\delta} C^{3}_{\alpha\beta\sigma\delta} \left(\overline{L_\alpha}\gamma^\rho \vec{\tau} L_\beta\right)\left(\overline{L_\sigma}\gamma_\rho \vec{\tau} L_\delta\right) \\ & + \ldots\end{aligned}$$

- Constraints are required to suppress unobserved large charged lepton transitions as $\mu \to 3e$. [see: Gavela, Hernandez, Ota, Winter, PRD 79 (2009) 013007]

- Phenomenological analysis: free NSI ε couplings.

NSI Effects on Oscillations

- Standard oscillations with matter effects:

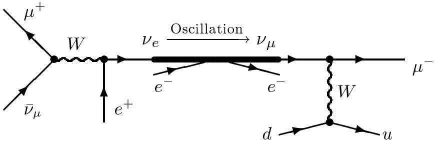

- NC NSI in neutrino propagation in matter $\sim \varepsilon$:

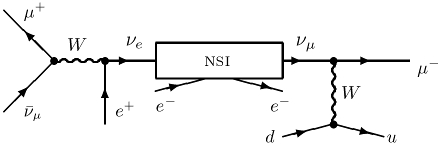

- CC NSI in neutrino production and detection $\sim \varepsilon^2$:

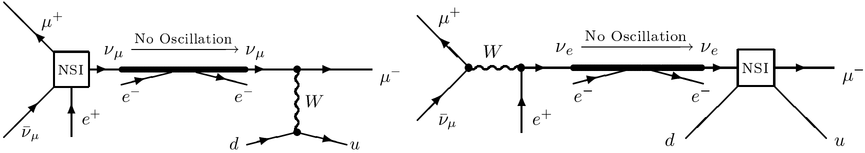

[Kopp, Lindner, Ota, PRD 76 (2007) 013001]

Neutrino flavor evolution equation in matter with NSI: $(\Delta_{kj} = \Delta m^2_{kj}/2E)$

$$
i\,\frac{d}{dx}\begin{pmatrix}\nu_e\\ \nu_\mu\\ \nu_\tau\end{pmatrix} = \left[U \begin{pmatrix}0 & 0 & 0\\ 0 & \Delta_{21} & 0\\ 0 & 0 & \Delta_{31}\end{pmatrix} U^\dagger + \sum_{f=e,u,d} V_f \begin{pmatrix}\delta_{ef}+\varepsilon^f_{ee} & \varepsilon^f_{e\mu} & \varepsilon^f_{e\tau}\\ \varepsilon^{f*}_{e\mu} & \varepsilon^f_{\mu\mu} & \varepsilon^f_{\mu\tau}\\ \varepsilon^{f*}_{e\tau} & \varepsilon^{f*}_{\mu\tau} & \varepsilon^f_{\tau\tau}\end{pmatrix}\right] \begin{pmatrix}\nu_e\\ \nu_\mu\\ \nu_\tau\end{pmatrix}
$$

unpolarized matter: $\varepsilon^f_{\alpha\beta} = \varepsilon^{fL}_{\alpha\beta} + \varepsilon^{fR}_{\alpha\beta}$ vector couplings

Global Analysis of Neutrino Oscillation Data

[Gonzalez-Garcia, Maltoni, JHEP 1309 (2013) 152; Gonzalez-Garcia, Maltoni, Schwetz, NPB 908 (2016) 199]

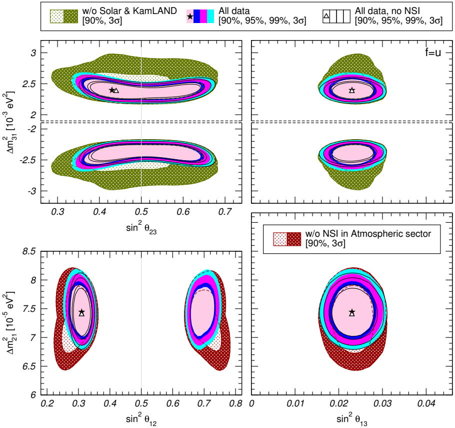

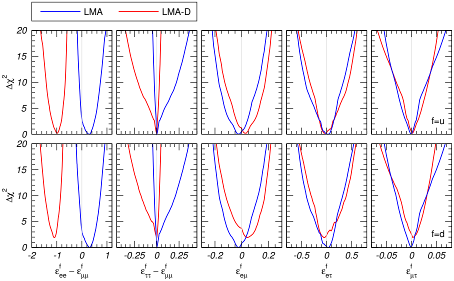

- "Dark-Side" LMA-D with $\vartheta_{12} > 45^\circ$ and large NSI. [Miranda, Tortola, Valle, JHEP 0610 (2006) 008]
- NSI have small effects on the determination of the other mixing parameters.

Neutrino NSI in CEνNS

- Effective NSI Hamiltonian:

$$\mathcal{H}_{\text{NSI}}^{\text{CE}\nu\text{NS}} = 2\sqrt{2} G_{\text{F}} \sum_{\alpha,\beta=e,\mu,\tau} \left(\overline{\nu_{\alpha L}} \gamma^{\rho} \nu_{\beta L} \right) \sum_{f=u,d} \varepsilon_{\alpha\beta}^{fV} \left(\overline{f} \gamma_{\rho} f \right)$$

- Axial NSI are negligible in CEνNS with heavy nuclei because the spin up and down contribution cancel.
- Only vector NSI, with $\varepsilon_{\alpha\beta}^{fV} = \varepsilon_{\beta\alpha}^{fV*} \Longrightarrow$ real ε_{ee}^{fV}, $\varepsilon_{\mu\mu}^{fV}$, $\varepsilon_{\tau\tau}^{fV}$
- NSI contributions to ν_{ℓ}–$\mathcal{N}$ CEνNS:

$$\frac{d\sigma_{\nu_{\alpha}\text{-}\mathcal{N}}}{dT}(E,T) = \frac{G_{\text{F}}^2 M}{\pi} \left(1 - \frac{MT}{2E^2} \right) Q_{\alpha}^2$$

- Weak charge:

$$Q_{\alpha}^2 = \left[\left(g_V^p + 2\varepsilon_{\alpha\alpha}^{uV} + \varepsilon_{\alpha\alpha}^{dV} \right) Z F_Z(|\vec{q}|^2) + \left(g_V^n + \varepsilon_{\alpha\alpha}^{uV} + 2\varepsilon_{\alpha\alpha}^{dV} \right) N F_N(|\vec{q}|^2) \right]^2 + \sum_{\beta\neq\alpha} \left| \left(2\varepsilon_{\alpha\beta}^{uV} + \varepsilon_{\alpha\beta}^{dV} \right) Z F_Z(|\vec{q}|^2) + \left(\varepsilon_{\alpha\beta}^{uV} + 2\varepsilon_{\alpha\beta}^{dV} \right) N F_N(|\vec{q}|^2) \right|^2$$

- Flavor-diagonal NSI interaction add coherently to weak interactions.
- Antineutrinos have the same cross section, because

$$g_V^f \to -g_V^f \quad \text{and} \quad \varepsilon_{\alpha\beta}^{qV} \to -\varepsilon_{\alpha\beta}^{qV}$$

- COHERENT: flux of ν_e, ν_μ, $\bar{\nu}_\mu$ $\Longrightarrow$ $\begin{cases} \text{Initial flavor: } \alpha = e, \mu \\ \text{Final flavor: } \beta = e, \mu, \tau \end{cases}$

- 10 effective NSI couplings: $\begin{cases} \varepsilon_{ee}^{uV} \quad \varepsilon_{\mu\mu}^{uV} \quad \varepsilon_{e\mu}^{uV} = \varepsilon_{\mu e}^{uV*} \quad \varepsilon_{e\tau}^{uV} \quad \varepsilon_{\mu\tau}^{uV} \\ \varepsilon_{ee}^{dV} \quad \varepsilon_{\mu\mu}^{dV} \quad \varepsilon_{e\mu}^{dV} = \varepsilon_{\mu e}^{dV*} \quad \varepsilon_{e\tau}^{dV} \quad \varepsilon_{\mu\tau}^{dV} \end{cases}$

$$F_u(|\vec{q}|^2) = \left(2ZF_Z(|\vec{q}|^2) + NF_N(|\vec{q}|^2)\right)$$
$$F_d(|\vec{q}|^2) = \left(ZF_Z(|\vec{q}|^2) + 2NF_N(|\vec{q}|^2)\right)$$

$$Q_e^2 = \left[g_V^p Z F_Z(|\vec{q}|^2) + g_V^n N F_N(|\vec{q}|^2) + \varepsilon_{ee}^{uV} F_u(|\vec{q}|^2) + \varepsilon_{ee}^{dV} F_d(|\vec{q}|^2)\right]^2 + \left|\varepsilon_{e\mu}^{uV} F_u(|\vec{q}|^2) + \varepsilon_{e\mu}^{dV} F_d(|\vec{q}|^2)\right|^2 + \left|\varepsilon_{e\tau}^{uV} F_u(|\vec{q}|^2) + \varepsilon_{e\tau}^{dV} F_d(|\vec{q}|^2)\right|^2$$

$$Q_\mu^2 = \left[g_V^p Z F_Z(|\vec{q}|^2) + g_V^n N F_N(|\vec{q}|^2) + \varepsilon_{\mu\mu}^{uV} F_u(|\vec{q}|^2) + \varepsilon_{\mu\mu}^{dV} F_d(|\vec{q}|^2)\right]^2 + \left|\varepsilon_{e\mu}^{uV} F_u(|\vec{q}|^2) + \varepsilon_{e\mu}^{dV} F_d(|\vec{q}|^2)\right|^2 + \left|\varepsilon_{\mu\tau}^{uV} F_u(|\vec{q}|^2) + \varepsilon_{\mu\tau}^{dV} F_d(|\vec{q}|^2)\right|^2$$

$$Q_\alpha^2 = \left[g_V^p Z F_Z(|\vec{q}|^2) + g_V^n N F_N(|\vec{q}|^2) + \varepsilon_{\alpha\alpha}^{uV} F_u(|\vec{q}|^2) + \varepsilon_{\alpha\alpha}^{dV} F_d(|\vec{q}|^2) \right]^2 + \sum_{\beta\neq\alpha} \left| \varepsilon_{\alpha\beta}^{uV} F_u(|\vec{q}|^2) + \varepsilon_{\alpha\beta}^{dV} F_d(|\vec{q}|^2) \right|^2$$

- NSI couplings with u and d quarks can cancel each other:

$$\varepsilon_{\alpha\beta}^{dV} = -\frac{F_u(|\vec{q}|^2)}{F_d(|\vec{q}|^2)} \varepsilon_{\alpha\beta}^{uV} \quad \Leftrightarrow \quad \varepsilon_{\alpha\beta}^{dV} \simeq -\frac{3.4}{3.8} \simeq -0.89\, \varepsilon_{\alpha\beta}^{uV} \quad \text{for CsI}$$

- Cancellations can be large, but not exact, because
  - Cs and I have slightly different $F_u(|\vec{q}|^2)/F_d(|\vec{q}|^2)$.
  - $F_u(|\vec{q}|^2)/F_d(|\vec{q}|^2)$ depends on $|\vec{q}|^2$, whereas $\varepsilon_{\alpha\beta}^{dV}/\varepsilon_{\alpha\beta}^{uV}$ is a constant.

- The diagonal NSI couplings can cancel the weak interaction contribution. Therefore, the signs are important for

$$\varepsilon_{ee}^{uV} \quad \varepsilon_{\mu\mu}^{uV} \qquad \varepsilon_{ee}^{dV} \quad \varepsilon_{\mu\mu}^{dV}$$

- The maximum contribution of each off-diagonal NSI coupling depend on its absolute value. Therefore, we can get bounds only on

$$|\varepsilon_{e\mu}^{uV}| \quad |\varepsilon_{e\tau}^{uV}| \quad |\varepsilon_{\mu\tau}^{uV}| \qquad |\varepsilon_{e\mu}^{dV}| \quad |\varepsilon_{e\tau}^{dV}| \quad |\varepsilon_{\mu\tau}^{dV}|$$

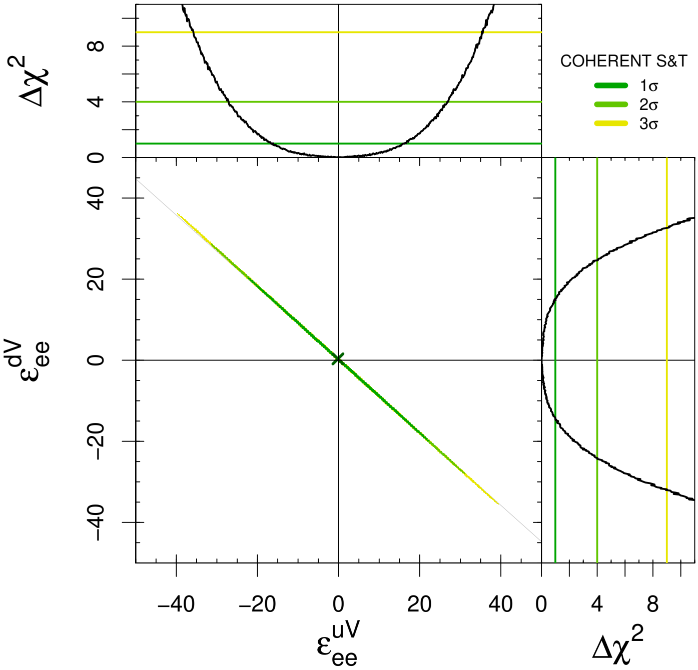

Δχ²
0
4
8
COHERENT S&T
1σ
2σ
3σ
ε_{ee}^{dV}
40
20
0
−20
−40
−40
−20
0
20
40
ε_{ee}^{uV}
0
4
8
Δχ²

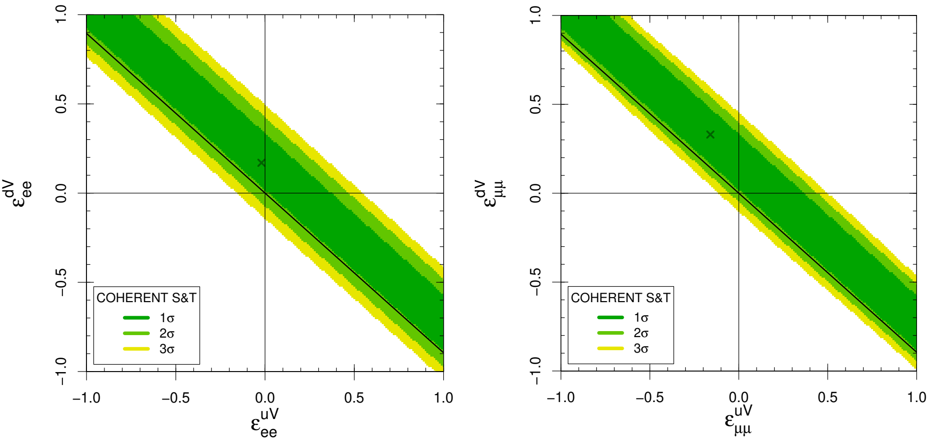

[Giunti, arXiv:1909.00466]

$$Q_\alpha^2 = \left[g_V^p Z F_Z(|\vec{q}|^2) + g_V^n N F_N(|\vec{q}|^2) + \varepsilon_{\alpha\alpha}^{uV} F_u(|\vec{q}|^2) + \varepsilon_{\alpha\alpha}^{dV} F_d(|\vec{q}|^2) \right]^2 + \sum_{\beta\neq\alpha} \left| \varepsilon_{\alpha\beta}^{uV} F_u(|\vec{q}|^2) + \varepsilon_{\alpha\beta}^{dV} F_d(|\vec{q}|^2) \right|^2$$

- Maximally constrained up-down linear combinations:

$$\widetilde{\varepsilon}_{\alpha\beta}^{V} \sim \frac{F_u(|\vec{q}|^2)\varepsilon_{\alpha\beta}^{uV} + F_d(|\vec{q}|^2)\varepsilon_{\alpha\beta}^{dV}}{F_u(|\vec{q}|^2) + F_d(|\vec{q}|^2)}$$

$$F_u(|\vec{q}|^2) = \left(2ZF_Z(|\vec{q}|^2) + NF_N(|\vec{q}|^2)\right) \approx (2Z+N)\,\overline{F}(|\vec{q}|^2)$$
$$F_d(|\vec{q}|^2) = \left(ZF_Z(|\vec{q}|^2) + 2NF_N(|\vec{q}|^2)\right) \approx (Z+2N)\,\overline{F}(|\vec{q}|^2)$$

$$\widetilde{\varepsilon}_{\alpha\beta}^{V} \sim \frac{(2Z+N)\,\varepsilon_{\alpha\beta}^{uV} + (Z+2N)\,\varepsilon_{\alpha\beta}^{dV}}{3\,(Z+N)}$$

- Cs: $(Z=55,\ N=78)$ and I: $(Z=53,\ N=74)$ $\Longrightarrow$ $(\overline{Z}=54,\ \overline{N}=76)$

$$\widetilde{\varepsilon}_{\alpha\beta}^{V} = \frac{3.4\,\varepsilon_{\alpha\beta}^{uV} + 3.8\,\varepsilon_{\alpha\beta}^{dV}}{7.2}$$

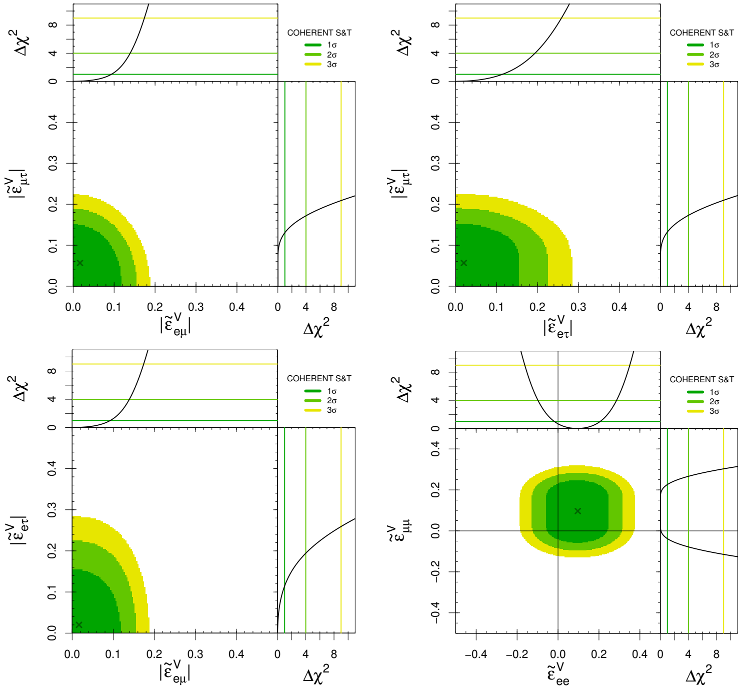
COHERENT S&T
1σ
2σ
3σ
Δχ²
$|\tilde{\varepsilon}^V_{\mu\tau}|$
$|\tilde{\varepsilon}^V_{e\mu}|$
$|\tilde{\varepsilon}^V_{e\tau}|$
$\tilde{\varepsilon}^V_{\mu\mu}$
$\tilde{\varepsilon}^V_{ee}$

NSI with up or down quarks only

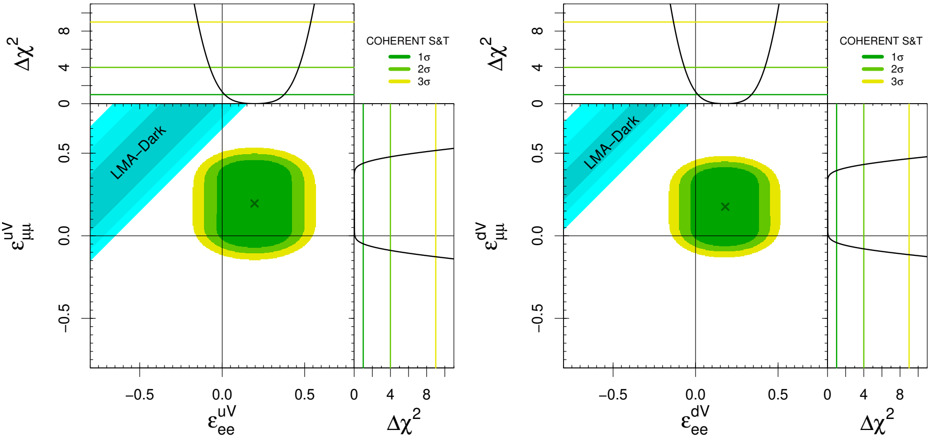

- LMA-Dark fit of solar neutrino data is excluded at:
  - 5.6σ for NSI with up quark only.
  - 7.2σ for NSI with down quark only.

[Giunti, arXiv:1909.00466]

Conclusions

- The observation of CEνNS in the COHERENT experiment opened the way for new powerful measurements of weak interactions, nuclear structure, and standard and non-standard neutrino properties:
  - Neutrino charge radii (SM and beyond).
  - Neutrino millicharges (beyond SM).
  - Neutrino magnetic moments (beyond SM).
  - Neutrino non-standard interactions (beyond SM).
  - Active-sterile neutrino oscillations (beyond SM).
  - ...

- COHERENT data constrain neutrino electromagnetic interactions, but are still not competitive with other measurements, except for the constraint on q_{ν_μ} that is the first one obtained from laboratory data.

- The new CEνNS experiments will improve the current constraints and maybe observe the neutrino charge radii predicted by the SM.

- There are several new experiments, most of which use reactor $\bar{\nu}_e$'s: CONUS, CONNIE, NU-CLEUS, MINER, Ricochet, TEXONO, νGEN

- It is important to continue and improve CEνNS observation not only with $\bar{\nu}_e$ from reactors, but also with ν_μ beams (as in COHERENT) in order to explore the properties of ν_μ, that are typically less constrained than the properties of ν_e in other experiments.

- New COHERENT observation of CEνNS with LAr detector.

- Interesting project at the European Spallation Source (ESS) in Lund, Sweden, with an order of magnitude increase in neutrino flux with respect to the SNS. [arXiv:1911.00762]